PHYSICAL MODELING OF PLUMES FROM COOLING-TOWER EMISSIONS--LIQUID AIR COMPANY, DENVER

by

M. Poreh,[1] W. W. Li,[2] J. A. Peterka[3]

and J. E. Cermak[4]

FLUID MECHANICS AND
WIND ENGINEERING PROGRAM

COLLEGE OF ENGINEERING

COLORADO STATE UNIVERSITY
FORT COLLINS, COLORADO

PHYSICAL MODELING OF PLUMES FROM COOLING-TOWER EMISSIONS--LIQUID AIR COMPANY, DENVER

by

M. Poreh,[1] W. W. Li,[2] J. A. Peterka[3]

and J. E. Cermak[4]

Sponsored by the
Colorado Department of Highways

Fluid Mechanics and Wind Engineering Program
Fluid Dynamics and Diffusion Laboratory
Department of Civil Engineering
Colorado State University
Fort Collins, Colorado 80523

CSU Project 2-96780

August 12, 1986

---

[1] Visiting Professor
[2] Research Associate
[3] Professor
[4] Distinguished Professor

CER86-87MP-WWL-JAP-JEC2

TABLE OF CONTENTS

LIST OF FIGURES

LIST OF TABLES

LIST OF SYMBOLS

Symbol		Dimension
A,B,n	constants	--
C	concentration of vapor at location interested	ppm
C_o	concentration of vapor at cooling tower exit	ppm
D	dilution factor, $D = C_o/C$	--
E	voltage	volt
e	fluctuating voltage	volt
F	buoyancy flux of plume, $\frac{g}{T_p}(T_p - T_e) WR^2$	--
g	gravitational acceleration	LT^{-2}
H	stack height	L
L	length scale	
M	momentum flux of plume, W^2R^2	--
P	porosity of wall	--
Q_o	exit discharge	L^3T^{-1}
R	radius of plume	--
s	plume traveling time	T
Te	ambient temperature	°K
T_p	plume temperature	--
U	local mean velocity	LT^{-1}
$U_{crit_{max}}$	upper bound of critical wind speed	LT^{-1}
$U_{crit_{min}}$	lower bound of critical wind speed	LT^{-1}
U_∞	ambient velocity at z = 139 ft	LT^{-1}
W	cooling tower exit velocity	LT^{-1}

Symbol		Dimension
W_a	external fans speed	LT^{-1}
WD	wind direction	degree
x,y,z	Cartesian coordinates	L
α	angle from the horizontal	degree
α'	constant	--
β	coefficient of momentum flux	--
Δz	effective plume rise	L

1. INTRODUCTION

This report describes a wind-tunnel study on the behavior of water-vapor plumes of cooling-tower emissions at the Liquid Air Company (LAC) in Denver. It has been established that, for northerly wind directions (WD = 280° to 20°) of moderate speeds, the vapor plumes emitted from the present configuration of cooling tower and surrounding buildings will impinge on the nearby viaduct, which is being built south of the cooling tower, and cause visual obscuration during the winter months. The relative location of the cooling tower and the viaduct are shown in Figs. 1 and 2. The purpose of the study is to identify possible structural configurations or devices which could eliminate or reduce the frequency of such visual obscurations.

The approximate behavior of the vapor plume was simulated in a 1:33.3 scale model at the Fluid Dynamics and Diffusion Laboratory (FDDL) of Colorado State University (CSU). The report outlines the criteria selected for the physical simulation as well as its limitations. It then classifies possible methods for eliminating or reducing visual obstruction on the highway, their effectiveness and limitations.

Almost one hundred different configurations were examined in the study. The behavior of the plume for the more efficient configurations was recorded on videotape, which forms an integral part of the report. Dilution ratios of the plume have also been measured for selected configurations.

Analysis of the data indicates that many configurations can significantly reduce the frequency of visual obscurations. The report provides the State Highway Department tools for comparing possible alternatives for reducing the potential of visual obscuration, according to their effectiveness and cost.

2. THE RATIONALE OF THE MODELING, SCALING CRITERIA AND LIMITATIONS

It is necessary to distinguish between the water-vapor plume, which may be visible or transparent to the human eye, and the visible plume in the atmosphere, which is the portion of the water-vapor plume that contains water mist due to vapor condensation.

Unless clearly specified, the term plume in this report will designate the entire water-vapor plume, which includes both its visible and its invisible portions. The plume seen in the videotape recorded in the wind-tunnel tests, which was generated by visible smoke, gives the approximate extent of the entire water-vapor plume. The visible plume in the atmosphere will always be smaller than the wind-tunnel plume, except for rare cases of fully saturated ambient conditions, where no evaporation at all is expected.

Two points should be clarified:

(1) The ability of the model to reproduce the entire plume.

(2) The expected dimensions of the visible plume.

The two points will be clarified with the aid of the ASHRAE Psychrometric Chart #6, reproduced in Fig. 3.

It is customary to assume that the plume leaving the cooling tower is fully saturated and that approximately an additional 1 g of liquid water is being carried with each kg of dry air in the form of droplets (Hanna et al., 1982, p. 76).

We shall assume, for example, that the dry-bulb temperature of the saturated plume at the exit is 24°C (75°F) (point (a) on the psychrometric chart). According to the chart, the plume will carry approximately 23 g/kg vapor and we shall thus neglect, for the sake of simplifying the discussion, the effect of the additional liquid phase

(5 percent) on the plume. We shall also assume in the example that the ambient air is at 0°C (32°F) and has a relative humidity of 80 percent (point (e) on the psychrometric chart). Mixing of the saturated air with the ambient air will reduce the temperatures of the plume according to the dilution (D). Here we define the local dilution as the water vapor concentration at the cooling-tower exit divided by the local concentration. If the plume is mixed with an equal amount of ambient air (D = 2), the average temperature of the plume will decrease to approximately 12°C, point (b) on the psychrometric chart. Clearly the plume will be over saturated and the condensation will produce a visible water mist. At this stage the air in the plume will be approximately described by point (c) on the chart. This condensation process heats the already hot plume and will slightly <u>increase</u> its plume rise. This process, however, is not reproduced in the model and thus the real plume is expected to be <u>slightly higher</u> than the simulated plume. The maximum error in plume rise, due to this approximation, has been estimated (Hanna et al., 1982) to be of the order of 30 percent. In our case it is expected to be much smaller, particularly at large wind speeds. If the initial plume contains a considerable amount of liquid water, in the form of fine droplets which have negligible settling velocities, the evaporation of these droplets will slightly increase the size of the visible plume and will slightly reduce its final buoyancy. In most cases, however, the contribution of the early condensation, which increases the buoyancy flux, is larger than the contribution of the additional droplets. Thus, the real plume rise will always be smaller than the simulated plume in the model. Moreover, since our study is aimed at finding a solution which will be acceptable for all wind

speeds, and not at reproducing the plume trajectory for a particular wind speed, the conservative estimate of the plume rise in the model is insignificant as far as the conclusions of the study are concerned.

Using the same chart one can also estimate at what dilution ratio the plume will become invisible. If the average dilution ratio is 15 the average plume will be approximately represented by point (d) on the line (a)-(e) in the chart, and the average relative humidity of the plume will be approximately 95 percent. At this point most of the visible plume should disappear. Since the actual mixing ratio in the center of the plume will be lower than the average dilution, the center of the plume might still be visible whereas the edges of the plume should become invisible much earlier.

For lower dry-bulb temperatures and higher relative humidities the dilution ratios required for the plume to become invisible will be larger. At times of fogging and a fully saturated atmosphere, dilution of the plume will not be very helpful, but of course visibility is already very poor in such cases. On the other hand, the frequency of such events is not very high, particularly when one refers to the outer edges of the plume.

Another effect should be taken into consideration at high dilutions. The distances among the droplets become large and one can see objects at moderate distances through the plume, as one sees through light fogs. Thus, even if a sizable portion of the water droplets could not evaporate, due to high relative humidities, at high dilutions the obscuration would be reduced.

Unfortunately, reliable statistical data on the joint probability distribution of wind speeds, temperatures and relative humidities at the site is not available. One cannot calculate the percentage of the time in which obscuration might occur as a function of the dilution. Thus, the performance of the tested configurations was initially evaluated on the basis of the visual observations of the simulated plume in the wind tunnel. The dilution ratio of the plume in the model was, however, measured for selected configurations. The measurements were consistent with the visual observations in the model. The State Highway Department is therefore encouraged to take into consideration the fact that the simulated conditions of a highly saturated atmosphere occur in the atmosphere infrequently, and that at high dilution rates obscuration is reduced, even in such cases.

The dimensionless plume trajectory is expected to be determined by the buoyancy flux (F), the momentum flux (M) at the exit of the plume (where M is proportional to the square of exit velocity), the ambient dimensionless velocity and turbulent fields, the geometry of the nearby structures, the cooling tower configuration, and the mode of the plant operation (Poreh et al., 1981). The dimensionless geometry of the region is represented in the model in a 1:33.3 scale. It is expected from our previous experience (Cermak, 1971) that the Reynolds number effects in the model are relatively small in the present study. Thus, for a given configuration the plume rise can be described by

$$\frac{z}{x} = f\left(\frac{F}{U^3 x}, \frac{M}{U^2 x^2}\right) = f\left(\frac{F}{U^3 x}, \frac{w^2 d^2}{U^2 x^2}\right)$$

where the functions f are identical in the model and prototype. When the effect of the nearby structures is small, the above relation is usually approximated by (Briggs, 1984),

$$\frac{\Delta z}{x} = \left(\alpha' \frac{F}{U^3 x} + \beta \frac{M}{U^2 x^2} \right)^{1/3}$$

where $\alpha' = 4.17$, $\beta = 0.4 + 1.2\ U/W$, and W is the initial exit velocity.

Two limiting cases can be identified. Close to the exit, small x, the momentum term (the second term) is dominating and the contribution of buoyancy (the first term) is negligible. The same is true for high wind speeds and moderate distances from the exit. Thus, when simulating the plume trajectory at high speeds, the value of F is insignificant. In fact, since the momentum term itself becomes small, $\Delta z/x$ becomes a function of the geometry only. On the other hand, for very low wind speeds and small exit velocities (when the cooling tower fans do not operate), the contribution of F becomes dominant.

Since the LAC cooling tower is expected to operate at a wide range of ambient wind conditions, it was decided to examine the trajectories of the plume for a continuous spectrum of wind speeds from almost zero wind speed, for which buoyancy dominates the plume rise, to very high wind speeds for which the plume trajectory becomes almost independent of the exit conditions. For these cases the exact scaling of the buoyancy flux or velocity in the model becomes irrelevant.

In cases where F is dominant, the scaling in the wind tunnel was determined so that $F/(U^3x)$ is the same in the model and prototype. In cases where F is not important, the scaling was determined so that W/U is the same in both the model and prototype.

One limitation of the present study is that it simulates the plume behavior in thermally neutral surface winds. Although the plant site may experience different kinds of thermal stratifications in the atmospheric boundary layer, the effect of the temperature stratification on the plume dispersion near the source is expected to be negligible. Hanna et al. (1982) concluded that stability has little influence at time period less than $s^{-1/2}$, where $s = g/T_e(\partial T_e/\partial z + 0.01\ ^\circ C/m)$, T_e is the temperature of the environment, z is the azimuth height, and g is the gravitational acceleration. Therefore, stability of the atmosphere is not expected to affect the flow close to the ground at short distance. One exception should be noticed, however. It is the case of a very strong inversion slightly above the highway. The simulation of such a case in the wind tunnel is very difficult and hardly justified, as it is a priori clear that the plume will be carried by the wind to the layer below the inversion level and obscure visibility on the highway. The use of external fans for mixing of the plume immediately downstream of the cooling tower, which is one of the alternatives studied, would be highly helpful in such cases.

3. CLASSIFICATION OF PLUME TRAJECTORIES

It is convenient to define three types of plume trajectories relative to the viaduct, as shown in Fig. 2.

I. Elevated and Rapidly Rising Plumes

Such plumes, usually formed at low wind speeds and high buoyancy flux and/or large initial momentum and/or elevated stacks, will rise above the level of the viaduct and will not obscure visibility.

II. Impinging Plumes

For any exit conditions, there is always a range of wind speeds (and wind directions) for which the natural plume will impinge on the viaduct and cause visual obscuration at low temperatures and high relative humidity. We shall refer to this wind speed range as the <u>critical wind speed range</u> and designate its limits by $U_{crit_{min}}$ and $U_{crit_{max}}$. Namely,

$$U_{crit_{min}} < U < U_{crit_{max}} .$$

It was estimated, on the basis of our model tests that when the cooling-tower fans do not operate, $U_{crit_{max}}$ is of the order of 15 ft/sec.

The values of both $U_{crit_{min}}$ and $U_{crit_{max}}$ increase when the cooling-tower fans operate.

III. Almost Horizontal Plumes

At high wind speeds, the plume rise is usually very small and the plume shape will be independent of both the initial conditions and the wind speed. In this regime, plumes emitted from the present LAC cooling tower will be carried under the viaduct and will not cause visual obstructions. When emitted from elevated stacks, the center of the plume will be approximately at the level of the exit.

4. EXPERIMENTAL FACILITIES AND INSTRUMENTATION

The Wind-tunnel Facility

The present investigation was performed in the Environmental Wind Tunnel (EWT) of the FDDL at CSU. Plan and elevated views of the tunnel are included in Fig. 4.

The EWT was designed specifically to study atmospheric flow phenomena. The tunnel is an open-circuit facility with a 2.25-to-1 contraction ratio driven by a 50 hp variable-pitch, variable-speed fan. The test section is 52 ft in length and 12 ft x 8 ft in cross section. The wind speed in the test section can be adjusted continuously from 0.2 to 50 ft/sec and the ceiling is adjustable in height for control of the pressure gradient. This wind tunnel is also equipped with transparent side walls and rotating turntables.

The Model

A circular area about the LAC, 400 ft in diameter, was modeled on a scale of 1:33.3 for use in the wind-tunnel study. The model was centered about the second cooling tower from the east.

All parts of the models, except the cooling tower fans, were fabricated within the FDDL from wooden and styrofoam materials and in the detail necessary to simulate prototype wind patterns around the LAC. All significant structures within the defined circular area were constructed in the model. In addition, some adjacent structures outside the 200 ft radius were constructed. Figure 5 shows the fabricated models in the EWT.

Velocity Measurements

Measurements of mean velocity and turbulence intensity profiles were obtained with a TSI Model 1050 constant temperature anemometer in conjunction with a TSI-10 quartz-coated cylindrical hot-film probe. The hot-film probe was calibrated with a TSI Model 1125 flow calibrator and an MKS Baratron Pressure Meter. Calibration data were fitted to the form of King's law,

$$E^2 = A + BU^n \ ,$$

using a least-square curve fitting program. The local turbulence intensity is obtained by a linear approximation, i.e.,

$$\frac{\sqrt{\overline{u_1^2}}}{U} = \frac{2E\sqrt{\overline{e^2}}}{nBU^{n-1}} \ .$$

A Datametrics Model 800LV linear flowmeter with probe was used to monitor the reference velocity in the EWT. The probe was placed at a height of 4.2 ft above ground throughout all measurements. The tunnel was set at various speeds according to the hot-film calibration results. An HP-2401 Integrating Digital Voltmeter was used to determine the Datametrics reading by integrating the signal over a 100-second interval. Hence, a calibration curve was obtained between the wind speed and the Datametrics reading. This curve then served as a reference for the mean wind speed throughout the experiment. Figure 6 shows the approaching velocity and turbulence profiles with a power law exponent of 0.15 which well represents an atmospheric boundary-layer flow in an open terrain.

Flow Visualization

Smoke was used to observe plume behavior over the nearby highway. The smoke was produced by passing the source gases through containers of titanium tetrachloride located outside the EWT and transported through the tunnel floor by means of a tygon tube terminating at a mixing chamber beneath the cooling towers. The mixing chamber was connected with five outlets such that the exit flux to each cooling tower was kept the same. A complete series of flow visualization study was recorded on a VHS format videotape. Table 1 tabulates specific test parameters/conditions which were documented on the videotape.

Concentration Measurements

Concentration data obtained in the present study included samples along the southern side of the viaduct, a horizontal array of samples elevated 10 ft across the viaduct and an array of samples along the center of the plume in the vertical direction at the southern side of the viaduct. All samples, 1/16 in cm ID, were constructed on a movable rake.

For each concentration measurement, up to 20 samples were simultaneously drawn in a period of two minutes to a 50-sample collection system. Two samplers were employed to monitor the level of background concentration. The sample draw rate was set to 1.2 cc/s which results in a draw velocity of 2 ft/s. The collection system is composed of fifty, 30 cc air-tight syringes mounted between two circular aluminum plates. A variable-speed motor raises a third plate which lifts the plungers of all 50 syringes simultaneously. Syringes were completely flushed to prevent residual concentrations accumulated from earlier runs before any sample was taken. The sampler was periodically calibrated to insure proper function of every check valve and tubing assembly.

A Hewlett-Packard Model 5700A gas chromatograph (GC) with flame ionization detector was used to determine the mean concentration of scalar tracers. The flame ionization detector functions on the principle that a DC voltage on a collector electrode is proportional to a charge produced by charged particles when organics burn in a hydrogen/air flame. Air samples tagged with tracer component (propane) were carried into a combustion column by an inert carrier gas, nitrogen. Tracers arrived at the flame at separate times due to the diffusive properties of different hydrocarbon mixtures in the column. The DC voltage output from the electrode was amplified by an electrometer and fed to a Hewlett-Packard Model 3380 integrator. Separate peaks on the integrator output can be identified as contents of different tracer gases. Flow rates of auxiliary gases (air, hydrogen and nitrogen) were selected to yield a maximum sensitivity of the instrument. Zero drift of the gas chromatograph due to the impurities in the carrier gas was corrected by subtracting the background from baseline values.

The gas chromatograph can measure samples with sensitivity down to picogram (10^{-12}) quantities. It was calibrated with a certified methane-ethane mixture of known concentration every four hours during the experiment. The maximum error expected from the gas chromatograph was found to be less than 0.12 percent.

A nominal 6.01 percent propane and nitrogen mixture was adopted as tracer in the concentration measurements. Additional helium was used to achieve the desired buoyancy. Gases were fully mixed before releasing from the cooling towers.

5. CLASSIFICATION OF SOLUTIONS FOR THE VISIBILITY PROBLEM

One should distinguish between two basic types of solutions.

1) Solutions in which the visual vapor plume disappears due to considerable dilution in the ambient air. Rapid mixing is naturally achieved at high wind speeds. However, as explained earlier, the disappearance of the visual plume also depends on the ability of the water mist to evaporate, namely the temperature and relative humidity of the ambient air. At very low temperature and high relative humidities the visual plume can persist for very long distances, although dilution will improve the visibility even without evaporation.

2) Solutions in which the plume trajectory is modified to avoid impingement on the viaduct. In such cases visual obstruction is eliminated even when mixing is not effective.

In addition, the alternative of eliminating the entire visual plume using a wet/dry cooling tower, which is not included in the scope of the present investigation, should also be considered.

Configurations aimed at modifying the plume trajectory and enhance dilution can be classified as follows. Comments on operation and effectiveness which accompany the classification are based on the model tests.

A. Passive configurations aimed at creating elevated or rapidly rising plumes at all wind speeds.

Possible configurations are: tall stacks or walls between the cooling tower and the viaduct. Such configurations were tested at relatively high wind speeds, for which they are less effective.

Inherent shortcomings of such configurations are usually:

(1) Water droplets emitted from the cooling tower (drift) can fall on the highway and cause icing.

(2) Since the thickness of the plume increases with the distance, the plume will eventually reach ground level at large distances. Dilution at this stage is usually very large. However, in rare cases of an almost saturated atmosphere, visual obscuration can occur.

B. Passive configurations aimed at channeling the plume under the viaduct.

Such configurations are less effective at low wind speeds. The influence of the exit conditions (fan on/off), the direction of the initial jet on the effectiveness of such configurations is critical.

Such configurations will also increase considerably the frequency of fogging downstream of the viaduct.

C. Passive configurations which eliminate impingement by increasing the plume rise at low wind speeds, but channel the plume under the viaduct at high wind speeds.

D. Semi-active configurations which eliminate impingement by modifying the initial direction of the plume according to the wind speed and direction.

E. External fans, with vertical axes, which increase plume rise (and mixing) at the critical wind speeds.

F. External fans, with horizontal axes, which carry the plume under the viaduct at the critical wind speed range.

<u>In principle, one could eliminate visual obscuration by any of the above methods</u>. However, the effectiveness and cost of different solutions will vary considerably. The choice between the various alternatives should be made by the State Highway Department according to its own criteria of the cost/effectiveness ratio and local constraints.

6. TESTED CONFIGURATIONS AND THEIR EFFECTIVENESS

Almost 100 configurations have been tested in the wind tunnel. Some of the configurations were found to be ineffective and were immediately discarded. The vapor plume trajectories for the more promising effective configurations were recorded on videotape which should be considered as an integral part of this report. The results of the tests are summarized below.

We have used the classification described in Section 5 to designate the nature of each configuration (for example, A_1, A_2 and B_1). The run numbers mentioned below refer to the run numbers on the videotape.

<u>Configuration A1</u> (Runs 2 and 7)

This configuration, see Fig. 7, includes five stacks approximately 8 ft in diameter, built above the cooling towers. Obviously, these solutions belong to type A, as defined in Section 5.

The variables in the testing of this configuration were:

(1) The height of the stacks (H)

(2) A porous vertical wall, porosity (P) = 30 percent, built under the viaduct

(3) A solid vertical wall built under the viaduct (P = 0)

(4) A 10 ft parapet on the southern rim of the highway

(5) Closing of the gap between the east and west-bound lanes.

The walls, the parapet and the closed gap should be long enough to cover the sector WD = 280° to WD = 30°.

The tests indicated that the entire vapor plume will rise above the highway for:

(1) H $\geq$ 60 ft above cooling tower exit combined with a 30 percent porous wall or a solid wall under the highway.

(2) H $\geq$ 80 ft.

Even at these heights, the lower edge of the vapor plume could reach intermittently the southern lane of the highway. However, the minimum average dilution at that location is estimated to be very large, approximately 36. Thus, only in very rare cases would the visual plume reach that point.

<u>Configuration A2</u> (Run 3)

This configuration, Fig. 8, consists of a tall wall south of the cooling tower. The tests indicated that this configuration is inferior to configuration A1, apparently because of the stronger eddy downstream the wall carries the plume toward the southern lanes of the highway.

<u>Configuration C1</u> (Run 4)

The basic element of this configuration is a horizontal platform adjacent to and at the same level as the highway. The platform decreases considerably the value of $U_{crit_{max}}$.

The platform itself was found to be ineffective for various operational modes. It became effective only when the width of the platform was increased to 29 ft, the gap between the east-bound and west-bound lanes was closed, two 10-ft parapets were constructed at the edge of the platform and at the southern rim of the highway, and a directional hood was installed over the cooling tower fans to deflect the plume under the viaduct when the cooling tower fans were operating, as shown in Fig. 9.

The solution was found to be effective for all wind directions. However, it is possible that isolated puffs of visible vapor could reach the roadway on rare occasions.

Configuration D1 (Run 5)

The configuration consists of a large box-like structure, which covers the cooling towers and terminates south of the cooling towers under the viaduct (Fig. 10). It was initially hoped that this configuration would be a passive one and replace configuration C1. It was found, however, that it became effective only when the shape of northern section of the roof, above the cooling tower, could assume one of three angles; $\alpha = +45°$, $\alpha = -45°$, and $\alpha = -90°$, where α is the angle from the horizontal.

At $\alpha = 45°$, the plume was diverted under the viaduct for most wind speeds. At very low wind speeds part of the plume emerged north of the cooling tower but the plume rise was very high.

To ensure effectiveness when the cooling tower fans operated, the angle of the moveable section had to be changed to $\alpha = -45°$, to deflect the plume.

At very small wind speeds and southerly wind directions the position $\alpha = -90°$ blocked the motion of relatively buoyant plumes under the highway and then rose rapidly up.

Configuration E (Run 6)

A series of seven fans (diameter 8 ft) with axes slightly off the vertical direction ($\alpha = 75°$) were used to increase the plume rise and rapidly mix the vapor with the environment as shown in Fig. 11a. Both plume rise and dilution were observed in the tests.

The role of mixing in such a solution is crucial and it is clear that unless considerable dilution is achieved the effectiveness of the solution could decrease when the ambient air will be very cold and humid. A detailed estimate of the dilution ratio for this alternative is given in the next chapter.

Configuration F (Run 6)

The use of external fans, placed north of the cooling towers, which blow toward the viaduct at a slight angle toward the ground, was found to be very effective (Fig. 11b).

Such fans should operate only when the winds blow toward the highway at speeds $U_{crit_{min}} < U_{\infty} < U_{crit_{max}}$. This solution will increase the percentage of time when the plume will pass under the highway and could increase the incidence of icing on the road under the highway. The plume will be blown toward businesses located on the ground south of the highway.

Note: The gap between the east-bound lanes and west-bound lanes south of LAC, should be closed in configurations E and F.

DILUTION RATES

The dilution is defined as the ratio C_o/C where C_o is the concentration of the vapor at the exit from the cooling tower and C is the concentration of the original vapor after mixing with the ambient air. In general

$$\frac{C_o Q_o}{CUL^2} = f\left(\frac{W}{U}, \frac{F}{U^3 L}\right)$$

where Q_o is the exit discharge, U the ambient velocity, L a length scale, W the exit velocity at cooling tower, and F the buoyancy flux.

For cases of very high wind speeds, the value of the function f becomes constant and C_o/C is proportional to U. Namely, dilution is high at high speeds and it decreases as wind speed decreases. At low wind speeds, however, the effect of either $F/(U^3L)$ or W/U is to increase the plume rise and thus increase the dilution.

For configuration A1, we have determined the value for high speeds and extrapolated the results to low speeds without taking into consideration the positive effect of either $F/(U^3L)$ or W/U of the cooling tower fans, as their values might change. Using this conservative approach, we have found that for Q_o = 5300 cfm and U_∞ = 7.5 ft/sec, the dilutions in the prototype for the worse point, which, 15 ft above the southern lane of the highway, are:

CONFIGURATION	DILUTION RATE
A1 - 60 ft stacks, WD = 330 (no wall)	24
A1 - 80 ft stacks, WD = 330 (no wall)	36
A1 - 80 ft stacks, WD = 285 (no wall)	36
WD = 15 (no wall)	23

The results are consistent with the observations in the wind tunnel, which suggested that a 60 ft stack would not be sufficient, whereas an

80 ft stack raises the plume such that only the very edge of the plume might from time to time reach the highway. The reader is encouraged to review again Run 7, to get an idea of what is the physical meaning of such a silution. As expected, at oblique angles the dilution was slightly reduced.

The dilution rate for the external fan configuration (E) at 10 ft above the southern lane, was determined by the equation

$$\frac{C_o Q_o}{CUL^2} = f\left(\frac{W_a}{U}\right)$$

where W_a is the exit velocity of the air from the external fans. The above function f was determined in the model for various values of W_a/U and the dilution C_o/C was calculated for Q_o = 53000 cfm and U = 6, 9, 12 and 15 ft/sec and are presented in Fig. 12. Due to the various limitations of the model and the need to resort to various approximations, it is recommended that the Line A in the figure be taken for design purposes, which gives <u>W = 90 ft/sec - a minimum dilution of 250</u>!

One may, of course, use either lower or higher values of W_a according to the desired dilution value. We recommend that W_a would be 90 ft/sec or more, as the savings from using smaller fans is estimated to be small.

7. CONCLUSIONS

Several configurations which could eliminate or significantly reduce the probability of visual obscuration on the viaduct south of the LAC cooling towers were identified. Each configuration has its own merits and drawbacks. The choice among the configurations must be made according to these merits and drawbacks, local constraints and the cost/performance ratio.

If cost is not taken into consideration, the expected dilution ratio may be considered as an important indication of the relative performance of the alternatives. Clearly, the performance of a dry/wet cooling tower would be the best, as it fully eliminates the visual plume and deposit of drift which could increase icing on the highway.

The second best solution is configuration E which uses almost vertical fans with exit speeds of 90 ft/sec or more. (The speed would have to be modified for different size fans to maintain the same momentum flux and a continuous air curtain.) In addition to the very high dilution achieved by the fans, they would reduce the deposit of drift on the highway, compared to other aerodynamic alternatives, and be very helpful in case of a slightly elevated inversion.

Configuration A1 (tall stacks) should also be considered as a possible solution, as it is a fully passive solution. The stack height of 80 ft above the present cooling-tower fans was recommended according to the visual observations in the model (see Runs 2 and 7 in the videotape). It was later found that the minimum dilution of the vapor at the edge of the plume near the highway for this height was 36, which suggests that such a dilution should be considered as a large dilution, although not as large as that achieved by the external fans. Of course higher dilutions can be achieved with higher stacks. Finally, since for oblique winds the dilution is slightly decreased, one might wish to consider even slightly higher stacks.

Unfortunately, lack of meteorological data does not permit correlation of dilution with the expected number of days in which visual obscuration will occur due to the LAC cooling tower above the number of natural obscurations due to fogs or storms. In our opinion, if large dilutions of the order of 250 are attained, the number of obscurations will not be increased significantly.

Other solutions which deflect the plume under the viaduct should be evaluated using different criteria. Criteria associated with possible problems under the viaduct and impact on areas south of the viaduct would require definition.

Finally, if any of the aerodynamic solutions identified is chosen, it is recommended that optimization of the final dimensions be made with the help of additional wind-tunnel tests.

ACKNOWLEDGMENTS

The important contribution to the investigation by J. L. Huckabay, from Environmental Research Consultants, Ltd., Denver, is gratefully acknowledged.

REFERENCES

1. Briggs, G. A. Plume Rise and Buoyancy Effects, (in Atmospheric Science and Power Production, Edited by D. Randerson) U.S. Department of Energy. DOE/TIC-27601, pp. 327-366, 1984.

2. Cermak, J. E. "Laboratory Simulation of Atmospheric Boundary Layer," AIAA J., Vol. 6, pp. 1746-1754, 1971.

3. Hanna, S. R., G. A. Briggs, and R. P. Hosker, Jr. Handbook on Atmospheric Diffusion. U.S. Department of Energy, DOE/TIC-11223, 1982.

4. Poreh, M. and A. Kacherginsky. "Simulation of Plume Rise in Small Wind-Tunnel Models," J. of Wind Engineering and Industrial Aerodynamics, Vol. 7, pp. 1-14, 1981.

FIGURES

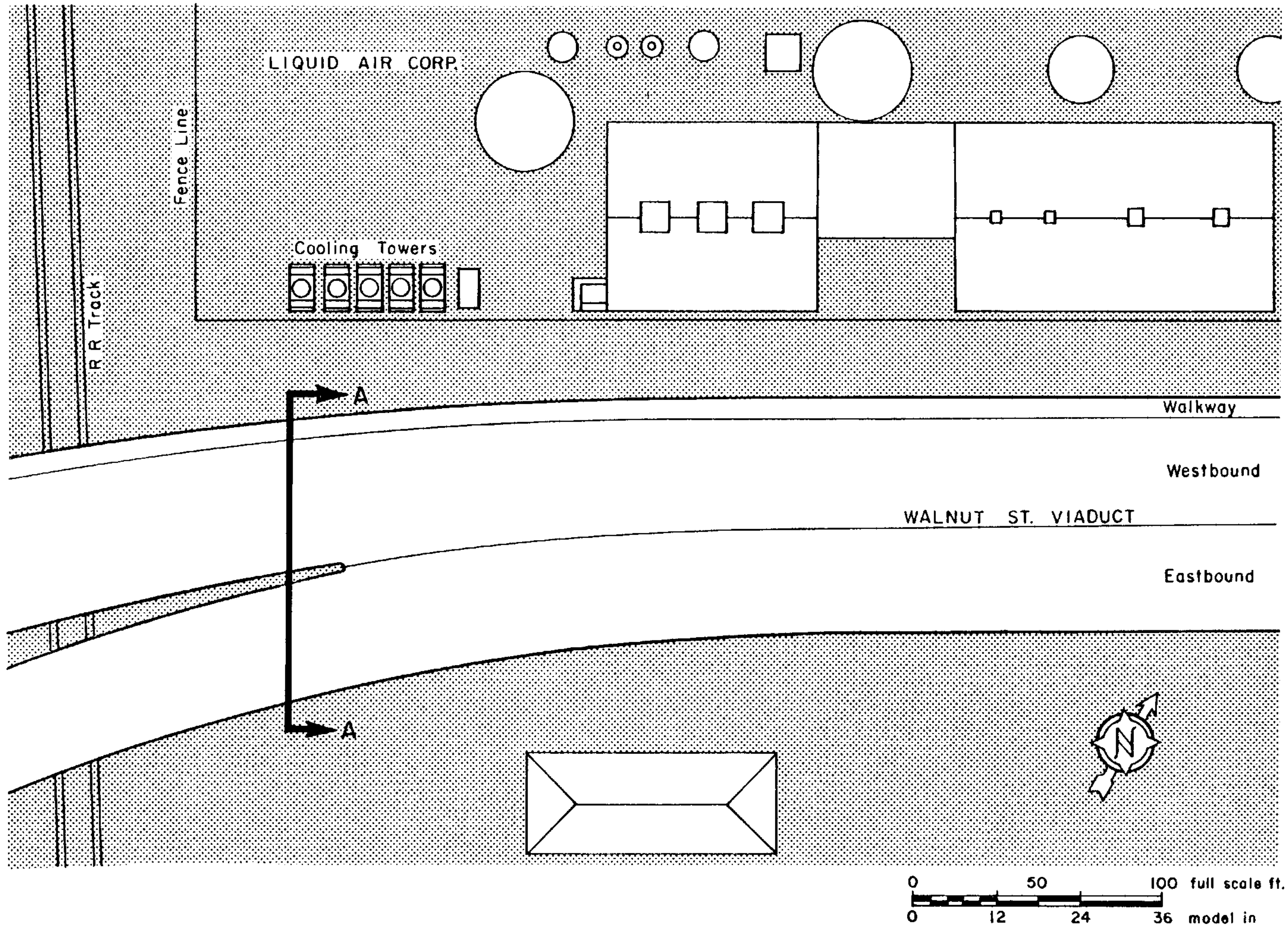

Figure 1. Plan View of LAC and Viaduct

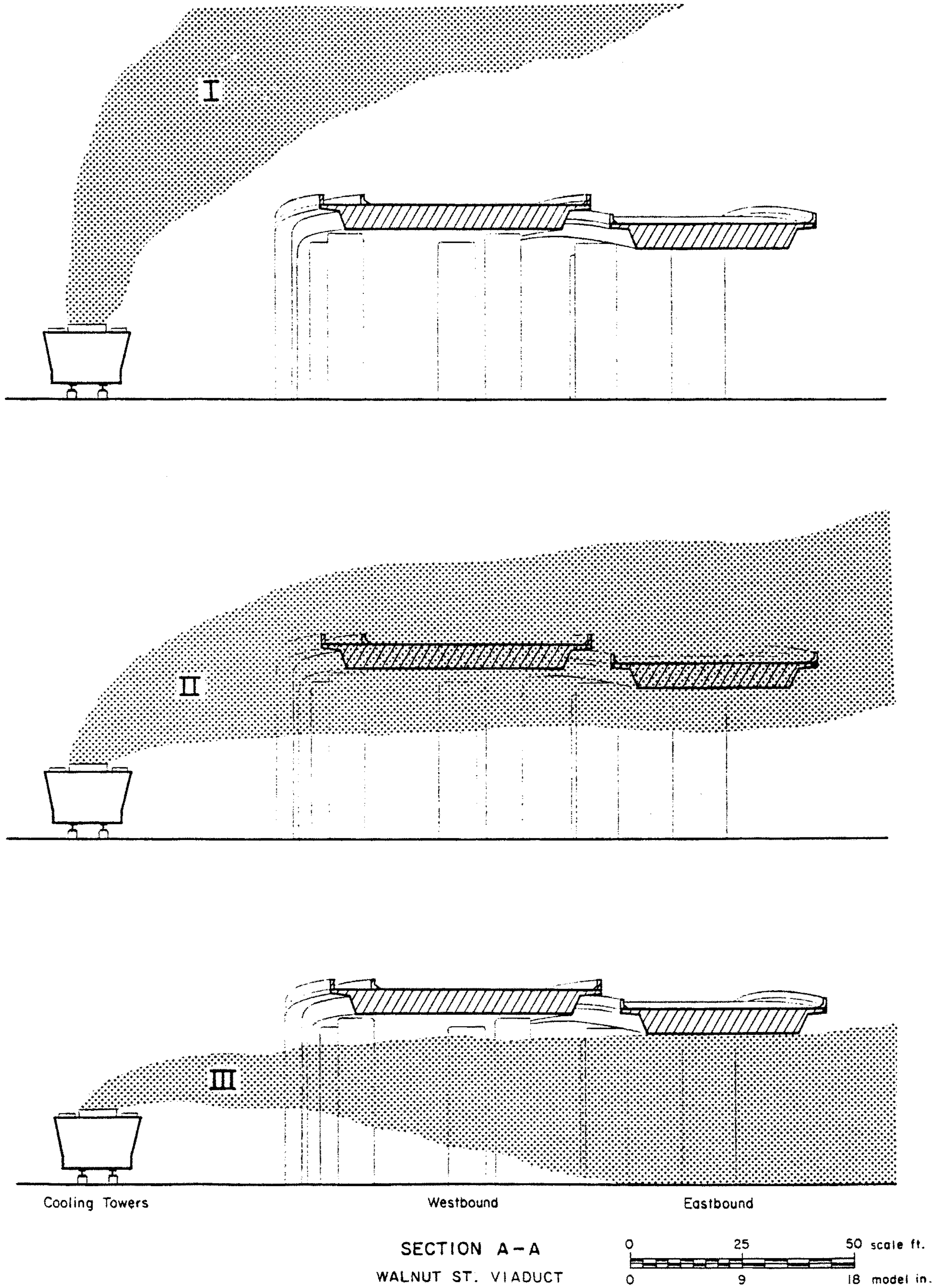

Figure 2. Typical Elevation and Types of Plume Trajectories

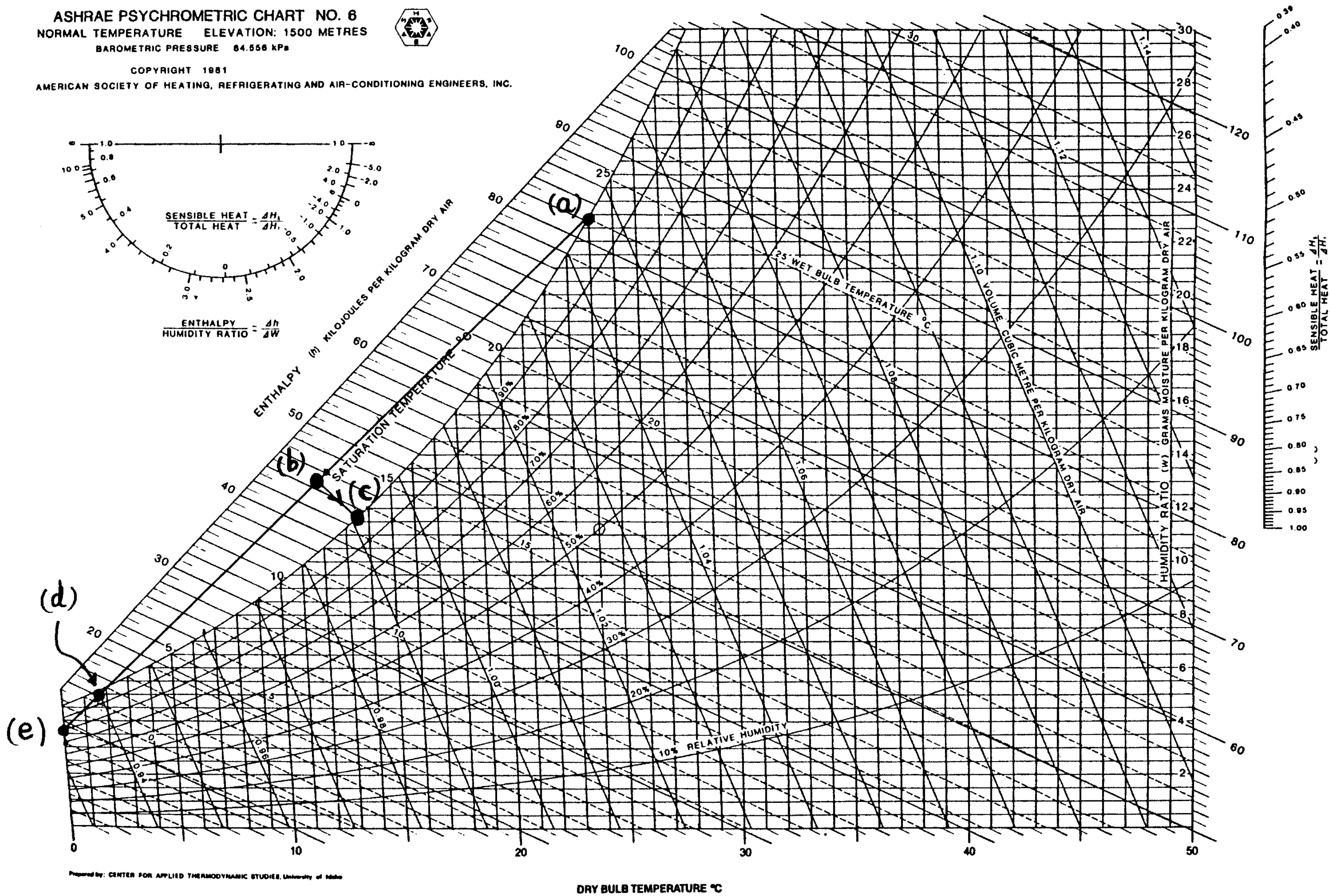

Figure 3. Psychrometric Chart for Elevation 1500 m

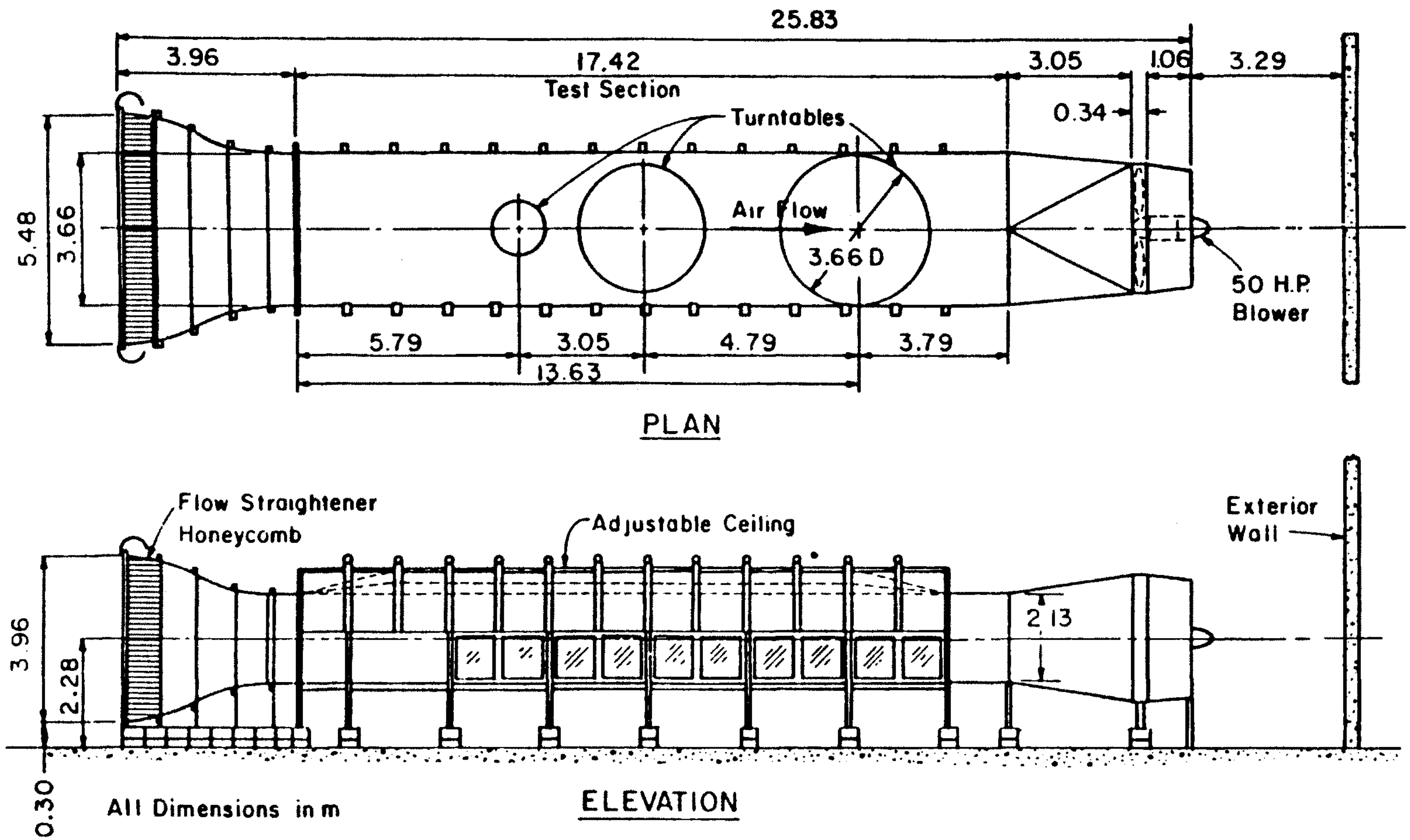

Figure 4. Plan and Elevation Views of the Environmental Wind Tunnel

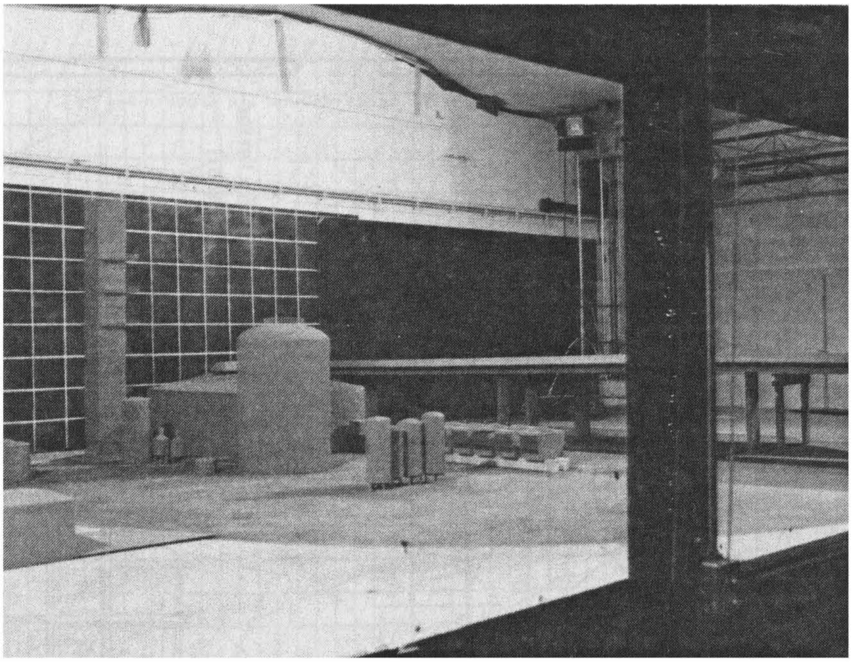

a) The LAC and nearby viaduct

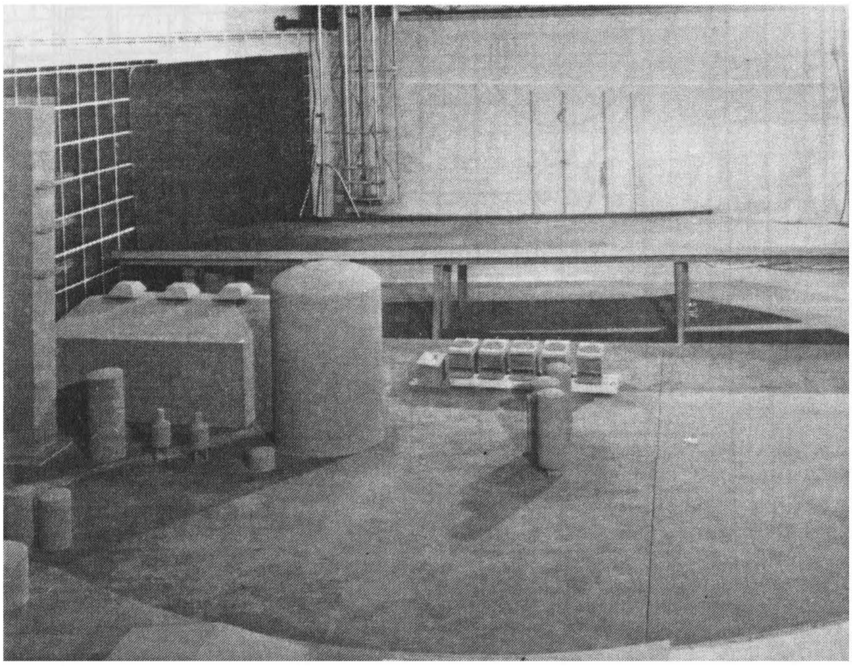

b) The LAC and nearby viaduct (closeup)

Figure 5. The LAC Models

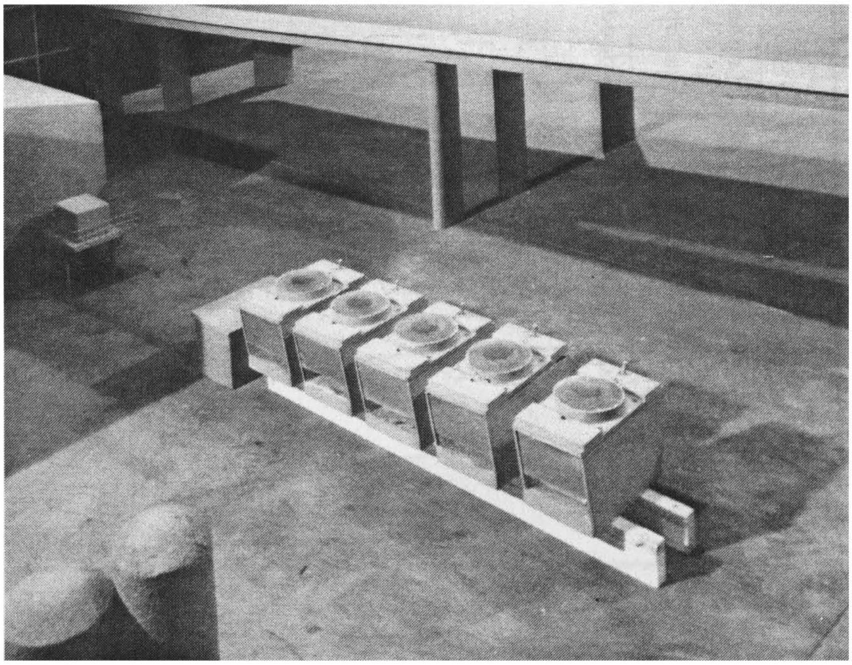

c) The LAC cooling tower

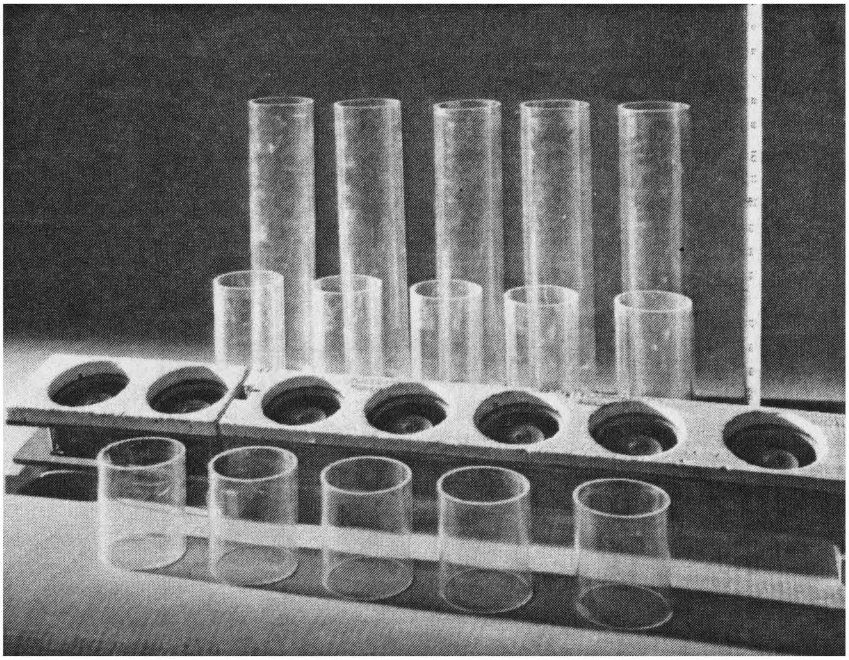

d) The stack attachments and external fans

Figure 5. The LAC Models (continued)

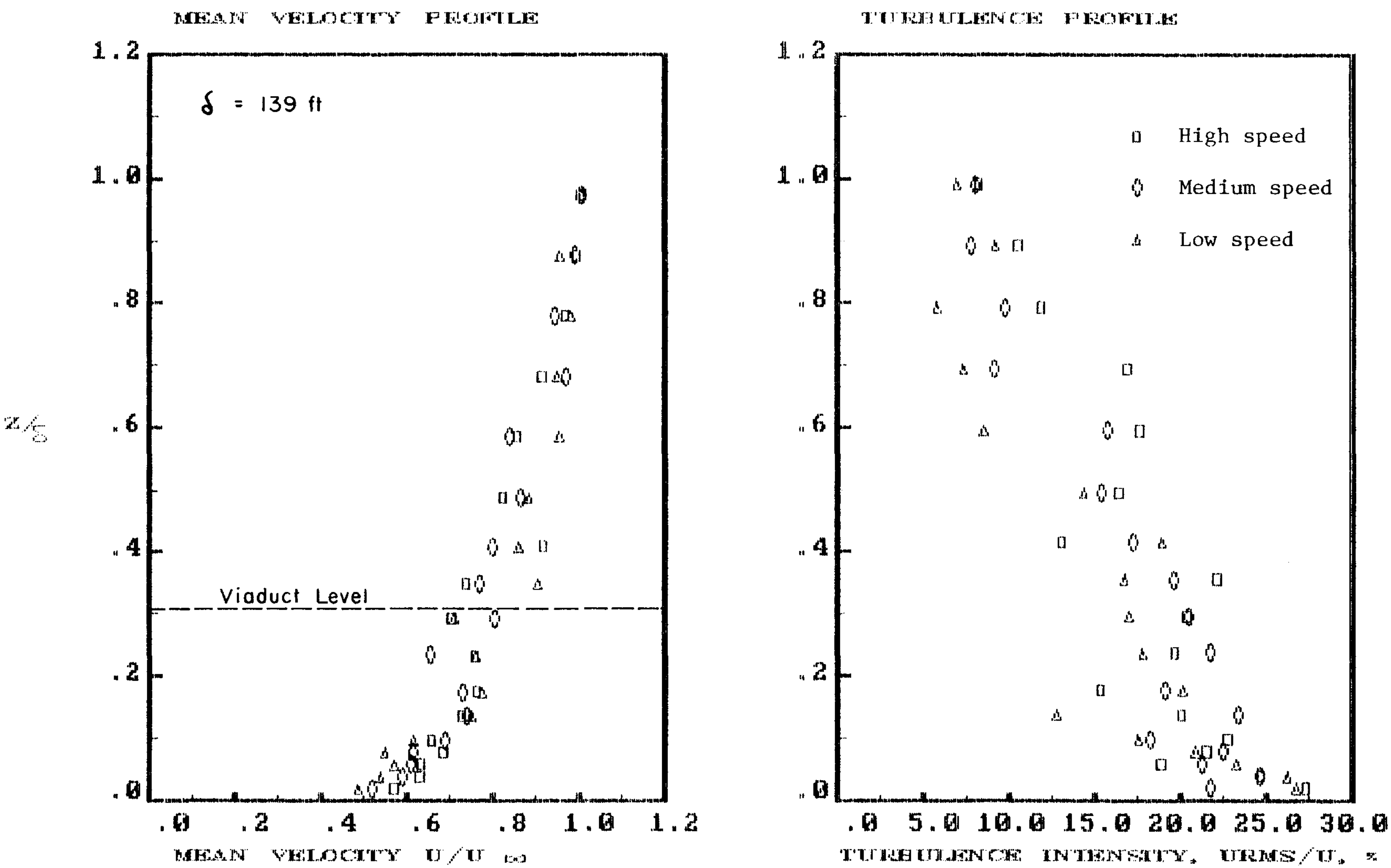

Figure 6. Mean Velocity and Turbulence Profiles Approaching the Model

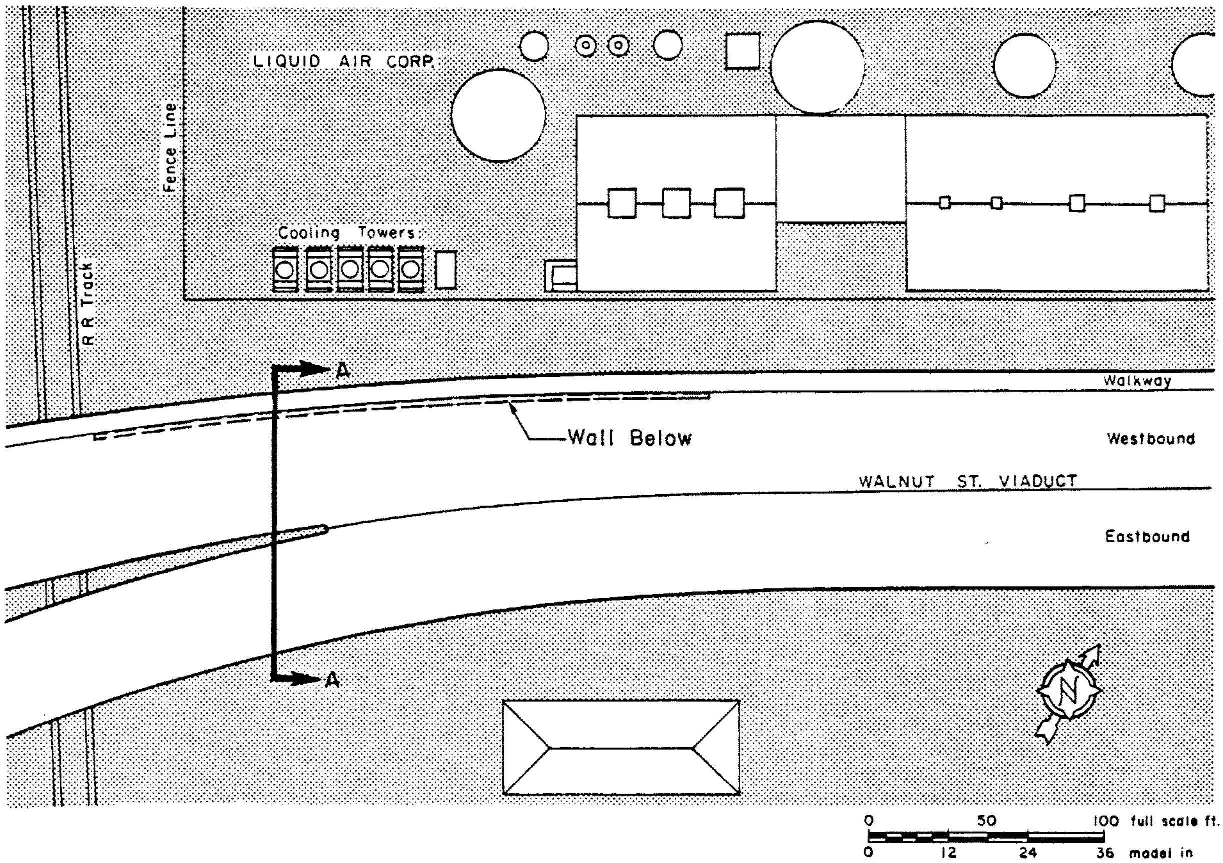

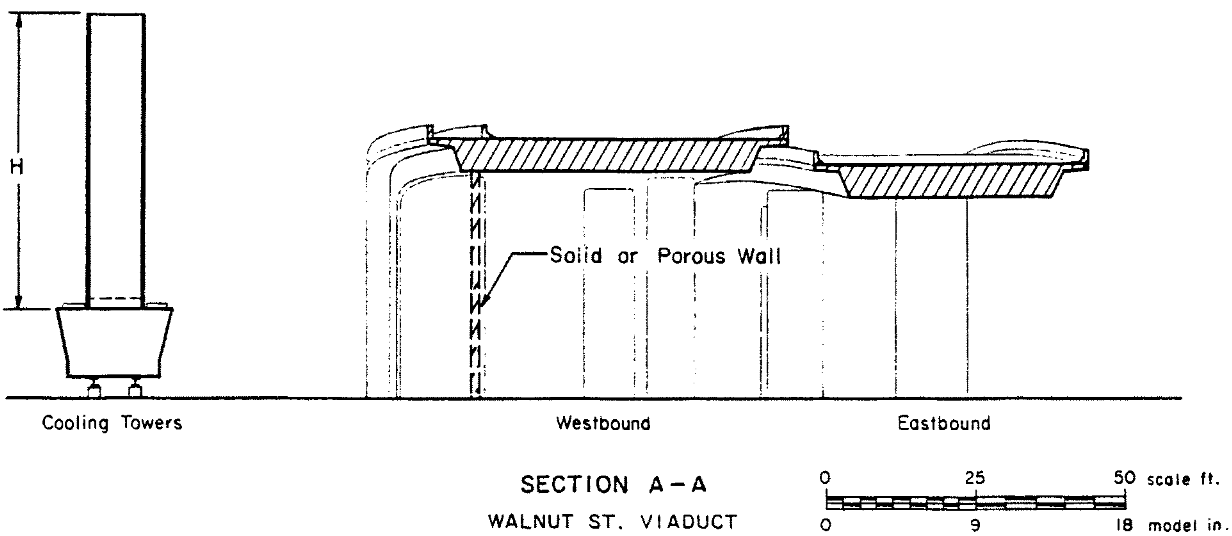

Figure 7. Configuration A1

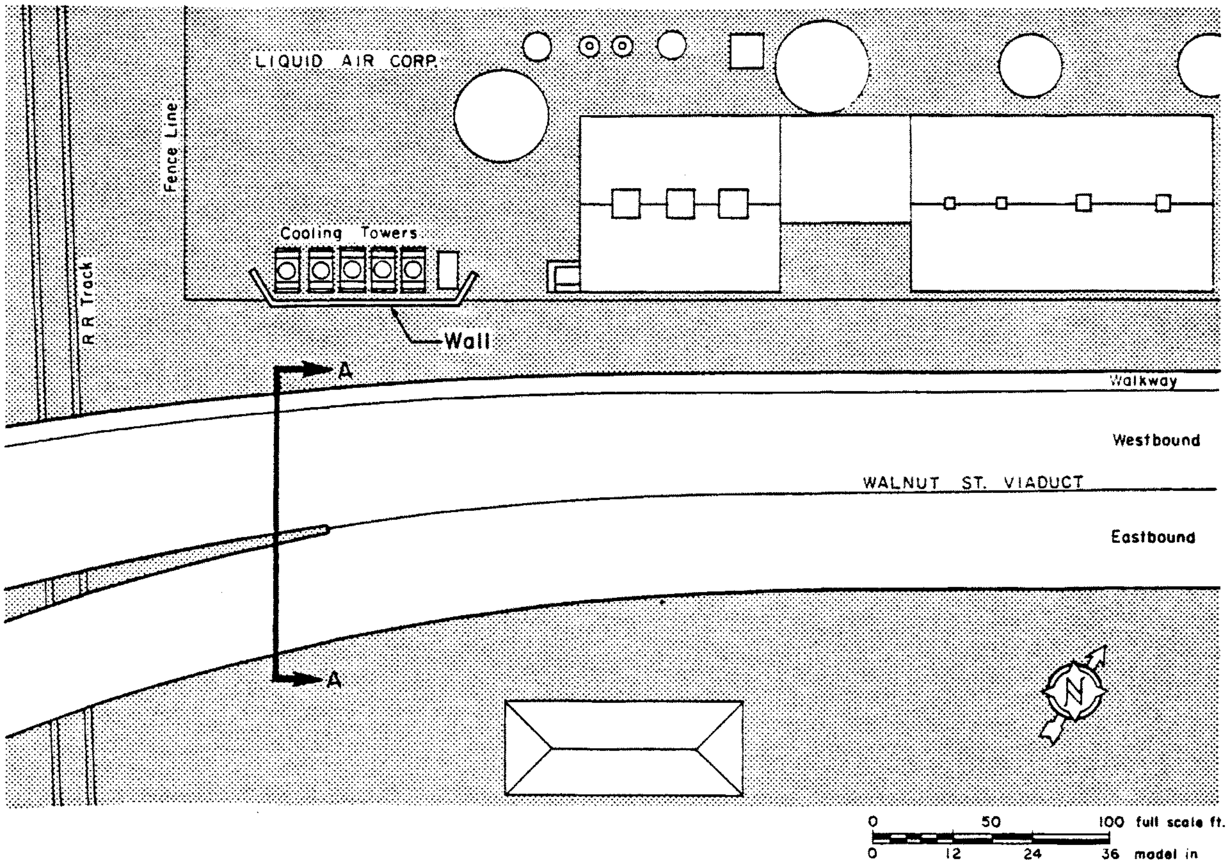

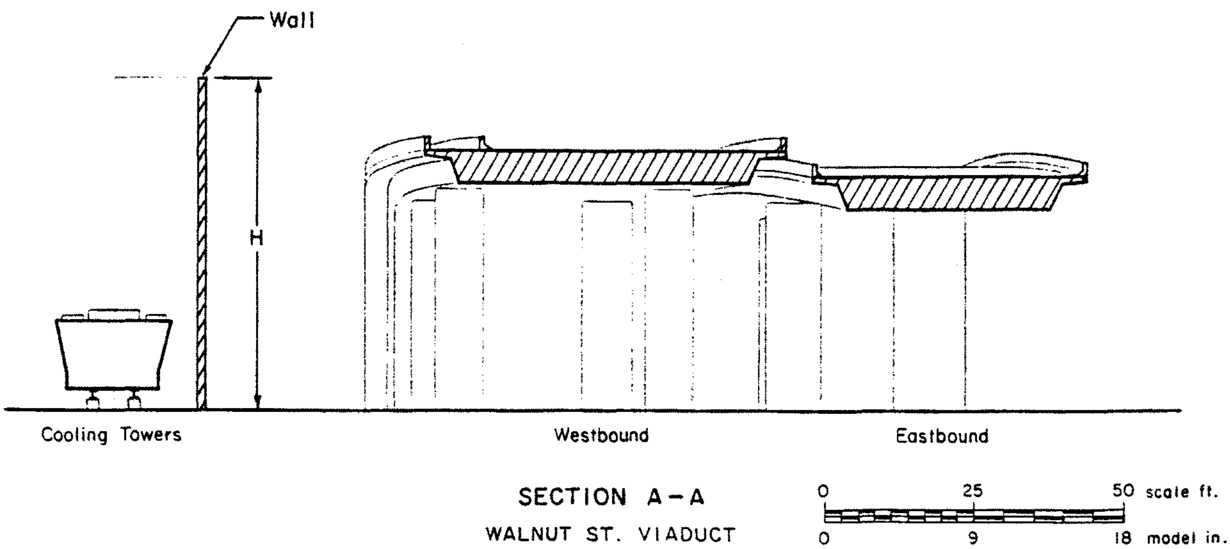

Figure 8. Configuration A2

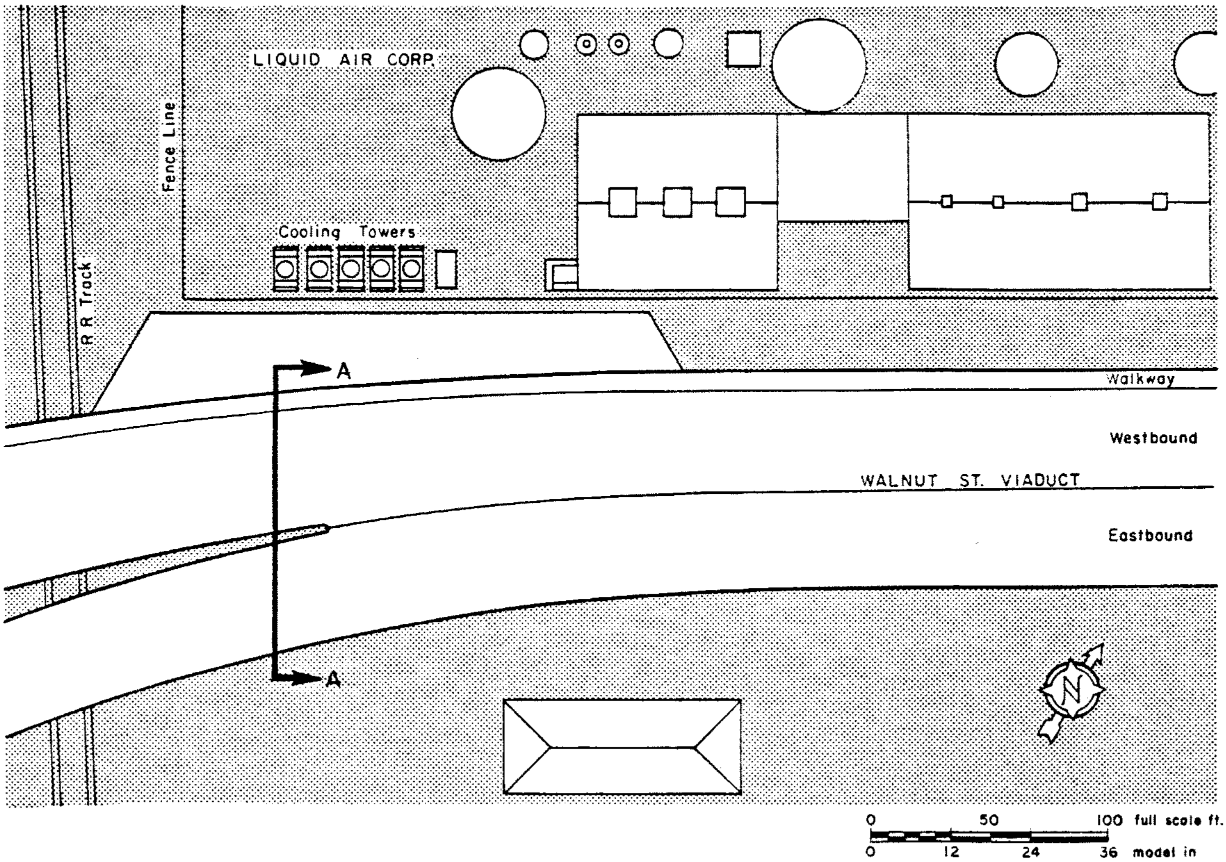

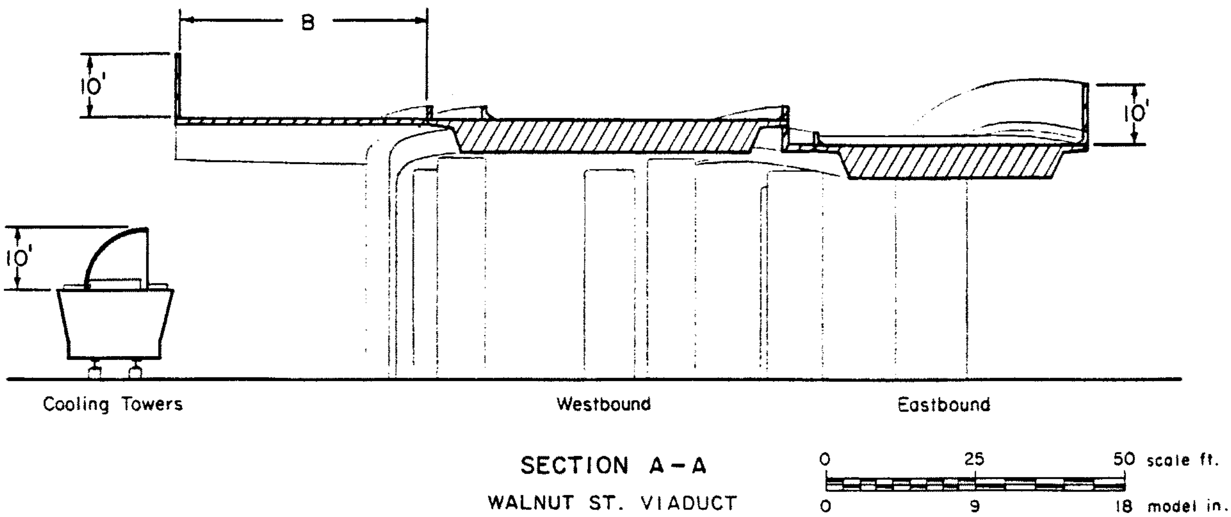

Figure 9. Configuration C1

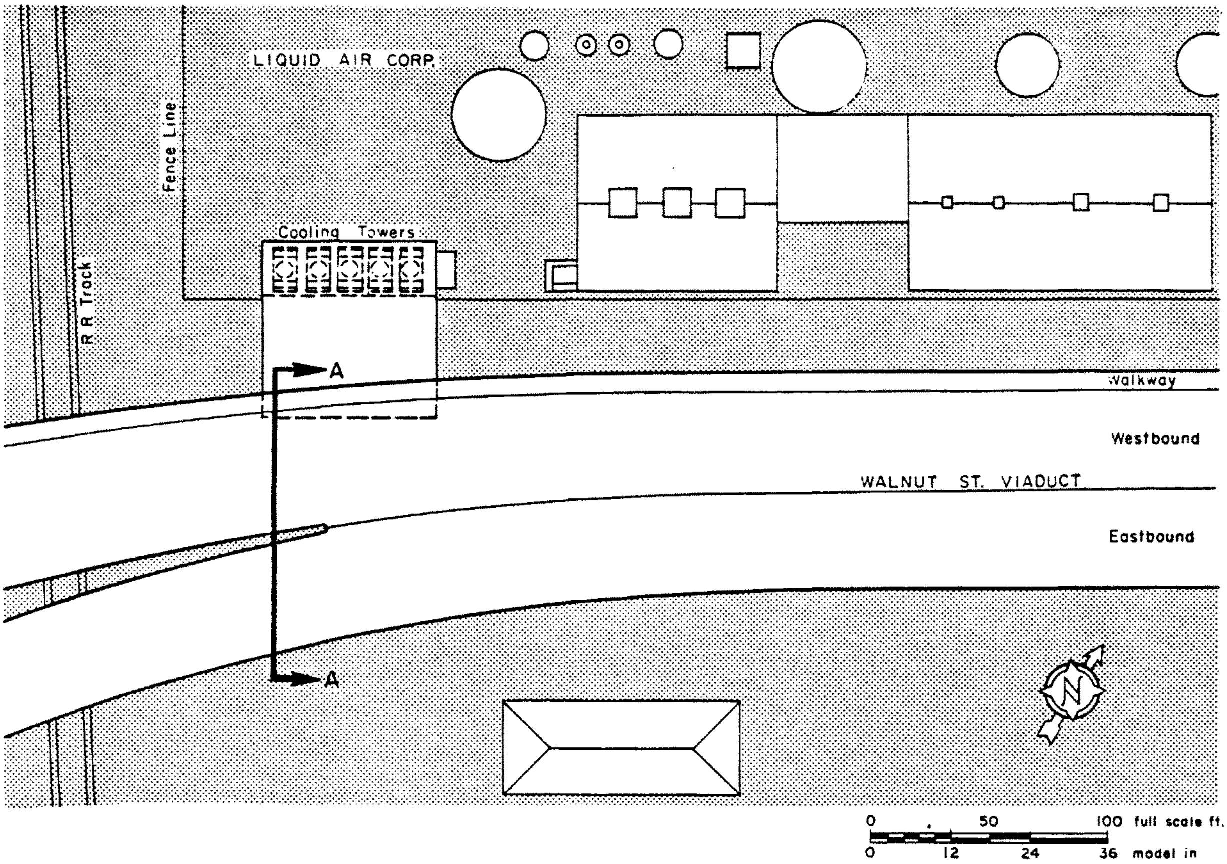

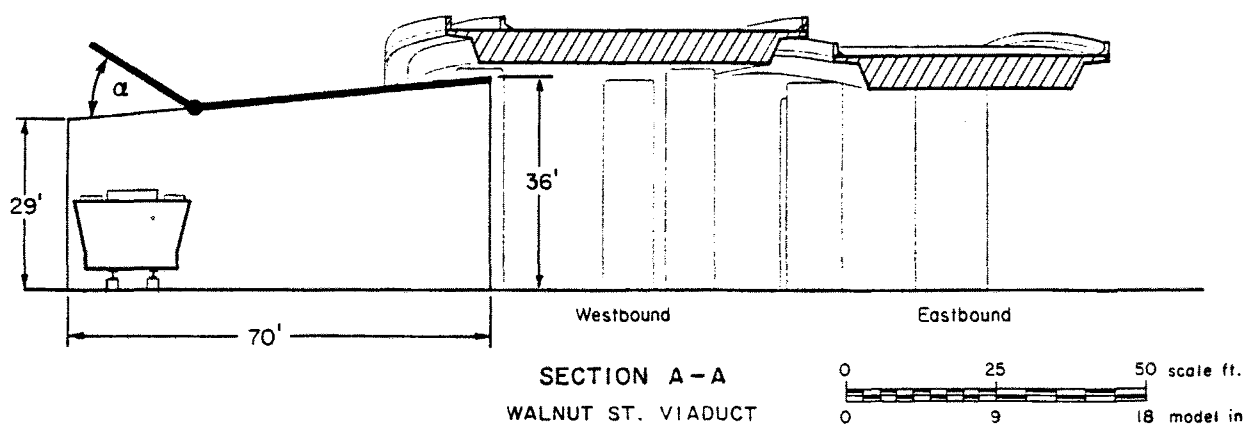

Figure 10. Configuration D1

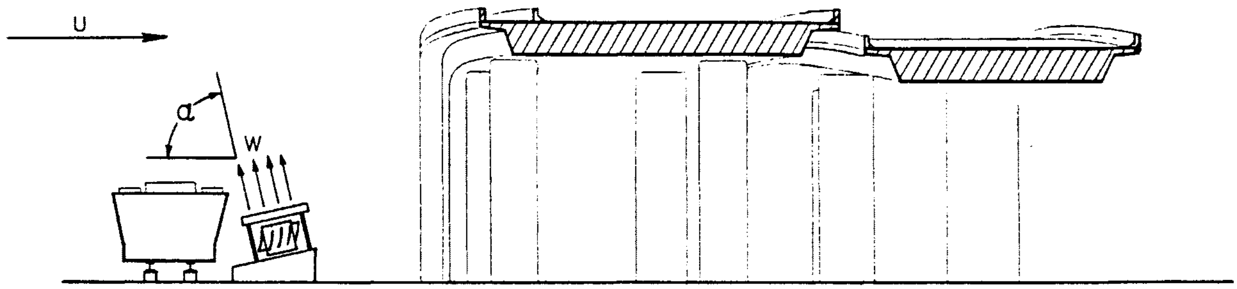

Figure 11a. Configuration E

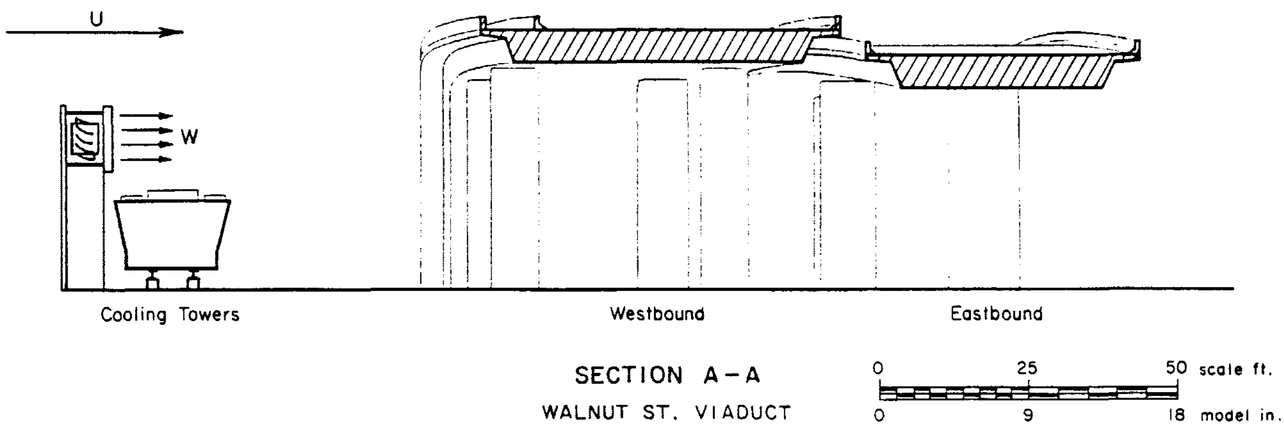

Figure 11b. Configuration F

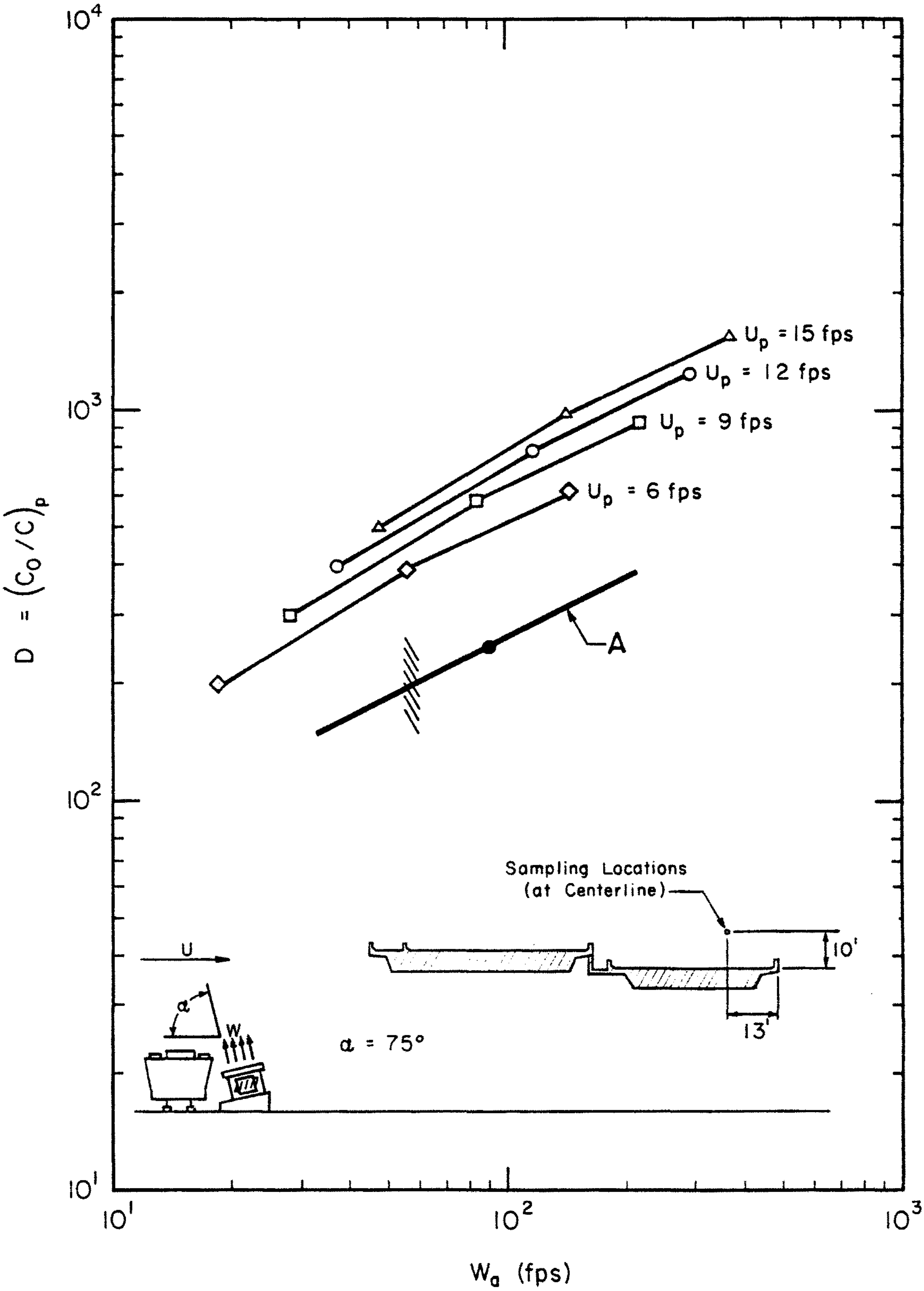

Figure 12. Prototype Dilution Values, Configuration E (for U = 15 ft/sec and U = 6 ft/sec)

TABLES

Table 1. Run Numbers and Test Configurations in Flow Visualization Study

Run No.	W.D.	Cooling Tower Fans	Configuration		
1	330	OFF	Existing plant configuration		
2	330	OFF	Stack Height, H(ft)	Porosity of a Wall Under Viaduct, P(%)	
2a	330	OFF	H = 20 ft	P = 100%	
2c	330	OFF	20	0	
2d	330	OFF	25	100	
2e	330	OFF	25	30	
2f	330	OFF	25	0	
2g	330	OFF	30	100	
2h	330	OFF	30	30	
2i	330	OFF	30	0	
2j	330	OFF	35	100	
2k	330	OFF	35	30	
2k(1)	330	OFF	35	30	Gap between lanes closed.
2m	330	OFF	35	0	
2m(1)	330	OFF	35	0	Gap between lanes closed.
2m(2)	330	OFF	35	0	Gap closed, 10 ft parapets on southern side of viaduct.
2n	330	OFF	H = 40 ft,	P = 100%	
2p	330	OFF	40	30	
2p(1)	330	OFF	40	30	10 ft parapets on southern side of viaduct. Gap closed.
2p(2)	330	OFF	40	0	
2p(3)	330	OFF	40	0	10 ft parapets on southern side of viaduct. Gap closed.

Table 1. (Continued).

Run No.	W.D.	Cooling Tower Fans	Configuration
3	330	OFF	Effect of a wall bewteen the plant and viaduct. Height of the wall, H High Wind Speeds
3a	330	OFF	H = 32.5 ft
3b	330	OFF	42.5
3c	330	OFF	52.5
3d	330	OFF	47.5
3e	330	OFF	37.5
4	330	On/OFF	Horizontal platform on northern side of viaduct at the level of the road width of platform, B. Wind speeds vary from high to zero during runs.
4a	330	OFF	B = 19 ft
4b	330	OFF	19 , 10 ft parapet on northern side of platform.
4c	330	OFF	19 , 10 ft parapet on northern side of platform.
4d	330	ON	19 , Directional hood on top of cooling towers.
4e	330	OFF	19 , Directional hood off, 10 ft parapet on southern side. Gap closed.
4f	330	ON	19 , Directional hood on, 15 ft parapet on southern side. Gap closed.
4g	330	OFF	19 , Directional hood on, 15 ft parapet on southern side. Gap closed.
4h	330	OFF	24 , Directional hood off, no parapet on southern side. Gap closed.
4i	330	ON	24 , Directional hood off, no parapet on southern side. Gap closed.
4j	330	OFF	24 , Directional hood off, 10 ft parapet on southern side. Gap closed.
4k	330	ON	24 , Directional hood off, 10 ft parapet on southern side. Gap closed.

Table 1. (Continued).

Run No.	W.D.	Cooling Tower Fans		Configuration
4m	330	OFF	24 ,	Directional hood on, 10 ft parapet on southern side. Gap closed.
4n	330	ON	24 ,	Directional hood on, 10 ft parapet on southern side. Gap closed.
4p	330	OFF	29 ,	Directional hood off, no parapet on southern side. Gap closed.
4q	330	ON	29 ,	Directional hood off, no parapet on southern side. Gap closed.
4r	330	OFF	29 ,	Directional hood off, 10 ft parapet on southern side. Gap closed.
4s	330	ON	29 ,	Directional hood off, 10 ft parapet on southern side. Gap closed.
4t	330	OFF*	29 ,	Directional hood on, 10 ft parapet on southern side. Gap closed.
4t(1)*	330	ON	29 ,	Directional hood on, 10 ft parapet on southern side. Gap closed.
4us	150*	ON	29 ,	Directional hood on, 10 ft parapet on southern side. Gap closed.
4v	150	ON	29 ,	Directional hood on, 10 ft parapet on both southern and northern sides.

*Error in the videotape.

Table 1. (Continued).

Run No.	W.D.	Cooling Tower Fans	Configuration
5	330	ON/OFF	Large duct above cooling towers. Width: 85 ft, Length: 70 ft Height of northern side: 29 ft; height of southern side: 36 ft Northern edge of the sloping roof can be adjusted according to the wind direction and mode of operation.
5a	330	OFF	Wind speed varies from high to minimum until the buoyant plume is not carried south of the viaduct. At this speed the shape of the northern section of the roof is modified.
			(i) High wind speeds
			(ii) Reduced wind speeds
			(iii) Very low wind speeds
			(iv) Very low wind speeds with new position of roof.
5b	330	OFF	Same as Run 5a except that the height of the northern* parapet is increased from 3 ft to 8 ft.
			(i) High wind speeds
			(ii) Reduced wind speeds
			(iii) Very low wind speeds
			(iv) Very low wind speeds with new position of roof.
5c	330	ON	Same as Run 5b except northern section of the roof tilted up.
			(i) Reduced wind speeds
			(ii) Reduced wind speeds, northern section of the roof is tilted to deflect the plume.
			(iii) Very low wind speeds
			(iv) Very low wind speeds, northern section of the roof is opened.
5d	---	OFF	The performance of Run 5b at various wind directions.
	280		(i) High wind speeds
	300		(ii) High wind speeds
	0		(iii) High wind speeds
	10		(iv) High wind speeds
	10		(v) Reduced wind speeds
	10		(vi) Very low wind speeds

Table 1. (Continued).

Run No.	W.D.	Cooling Tower Fans	Configuration
6	330	ON/OFF	Active plume control using auxiliary fans.
6a	330	OFF	Fans axes oriented 15 degrees off vertical
			(i) High wind speeds, auxiliary fans off
			(ii) Low wind speeds, auxiliary fans off
			(iii) Low wind speeds, auxiliary fans on
6b	330	ON	(i) High wind speeds, auxiliary fans off
			(ii) Low wind speeds, auxiliary fans on
6c	330	OFF	Auxiliary fans blowing toward viaduct horizontally.
			(i) High wind speeds, auxiliary fans off
			(ii) Low wind speeds, auxiliary fans off
			(iii) Low wind speeds, auxiliary fans on
			(iv) Low wind speeds, auxiliary fans off
			(v) Low wind speeds, auxiliary fans on
			(vi) Low wind speeds, auxiliary fans on but reduced by 50%
6d	330	ON	(i) High wind speeds, auxiliary fans off
			(ii) Low wind speeds, auxiliary fans on
			(iii) Low wind speeds, auxiliary fans on but reduced by 50%
7	330	OFF	Plume rise using tall stacks (Extension of Run 2)
7a			(i) H = 60 ft , P = 100%, with 10 ft southern parapet.
			(ii) 60 , 30
			(iii) 60 , 0
7b	330	OFF	(i) 60 , 100%, without southern parapet
			(ii) 60 , 30
			(iii) 60 , 0
7c	330	OFF	H = 60 ft , P = 100%, with 10 ft southern parapet
7d	330	OFF	60 , 100%, without southern parapet
7e	30	OFF	(i) H = 80 ft , P = 100%
	0	OFF	(ii) 80 , 100
	330	OFF	(iii) 80 , 100
	300	OFF	(iv) 80 , 100
	270	OFF	(v) 80 , 100
	255	OFF	(vi) 80 , 100